
Nonlinear Localized Interchange Mode and Current Sheet Formation

Ping Zhu

University of Wisconsin-Madison

In collaboration with C. R. Sovinec and C. C. Hegna

Questions

What is the consequence of the (nonlinear) localized interchange instability?

How/When does it lead/relate to enhanced (electron) transport, or disruptions?

Relevance

Advanced magnetic fusion devices operate in increasingly high- β and high- S regimes

(ITER, MST, W7AS, etc.)

Localized Interchange Mode and Suydam Criterion

- Localized Interchange Mode (LIM):
 - Interchange mode: pressure driven, $p' \kappa > 0$ and $k_{\parallel} = 0$
 - In magnetic configurations with shear, $k_{\parallel}(r_s) = 0$ only
 - LIM occurs near $r \sim r_s$. Near marginal stability,

$$\frac{\partial}{\partial x} \left(x^2 \frac{\partial \phi}{\partial x} \right) + \left(\frac{x}{r_s} \right)^2 (1 - m^2) \phi + D_I \phi = 0$$

where $x = r - r_s$, $D_I \equiv m^2 \beta' \kappa_r / (k'_{\parallel} r_s)^2$, and $k_{\parallel} = k'_{\parallel} x$

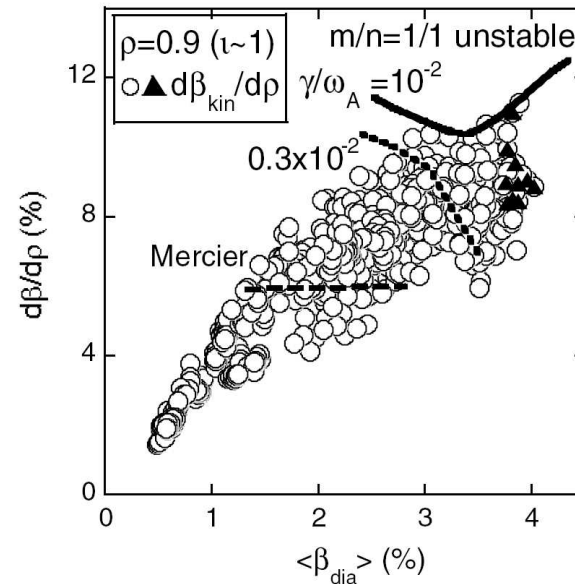
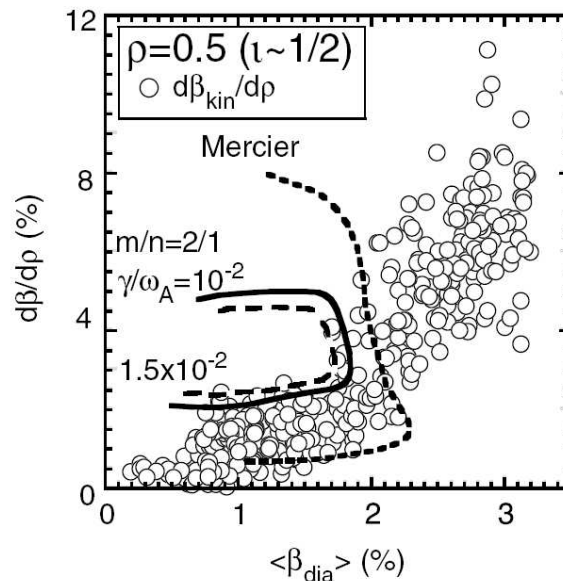
- Solution near $x = 0$ (regular singular point)

$$\phi = |x|^{-\frac{1}{2} \pm i\lambda} \sum_{i=0}^{\infty} A_i x^i \quad \text{where } \lambda = \sqrt{D_I - \frac{1}{4}}.$$

- Suydam's criterion:
 - $D_I > \frac{1}{4}$, oscillatory solution in x — Localized interchange mode
 - Stability requires $D_I < \frac{1}{4}$ (necessary condition).

Role of Nonlinear LIM Not Well Understood in Recent Experiments

- In DIII-D, electron heat transport different in interchange induced and kink induced sawtooth during reheat [Lazarus *et al.*, *Phys. Plasmas* (2007)].
- In LHD, Mercier criterion does not seem to restrict practical operational limits in β or β' [Watanabe *et al.*, *Nucl. Fusion* (2005)].



- In MST during PPCD discharges, Suydam criterion not satisfied yet still stable [Wyman, *Plasma Physics Seminar*, UW-Madison, January 29, 2007].

Linear LIM Itself Seems Not Very Dangerous

Growth of linear LIM near marginal stability is exponentially small:

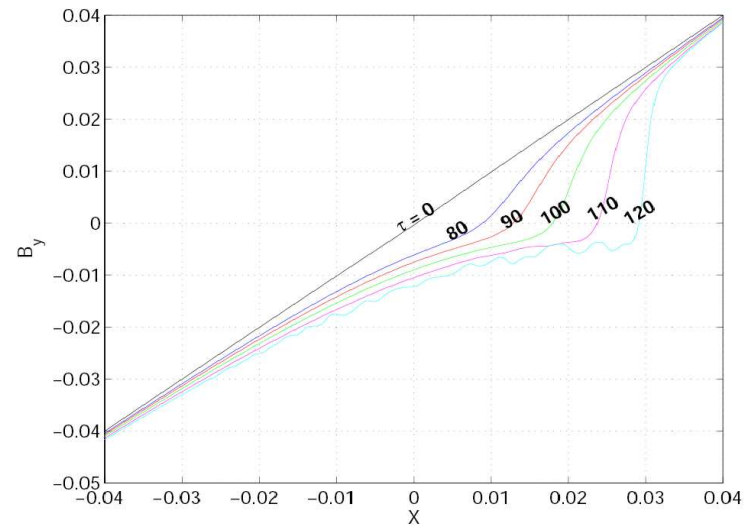
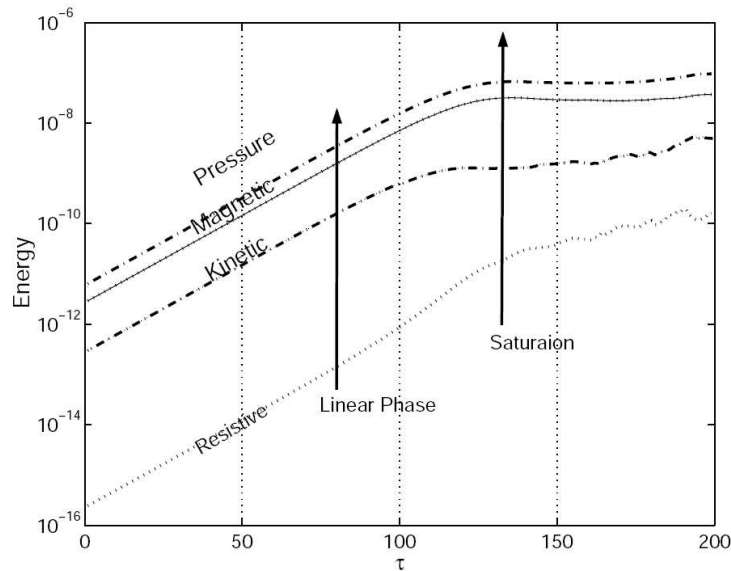
- Incompressible linear LIM [Gupta, Callen, and Hegna, *Phys. Plasmas* (2002)]
 - $1/4 < D_I < 0.5$: growth rate exponentially small; robust growth only after $D_I > 0.5$.
 - FLR stabilizes LIM for D_I up to about 0.5.
- Compressible linear LIM [Gupta, Callen, and Hegna, *Phys. Plasmas* (2005)]
 - Compressibility significantly reduces growth rate of LIM even for $D_I > 0.5$.

However, less localized interchange mode are more and most unstable.

- Violation of Suydam criterion guarantees the existence of gross interchange mode with larger growth [Goedbloed *et al.*, *Phys. Fluids* (1974)].
- In those linear studies, Gupta *et al.* only considered the growth of the most localized interchange mode ($\phi \sim |x|^{i\lambda}$, λ is real).

Nonlinear LIM: Reduced MHD Theory and Simulation

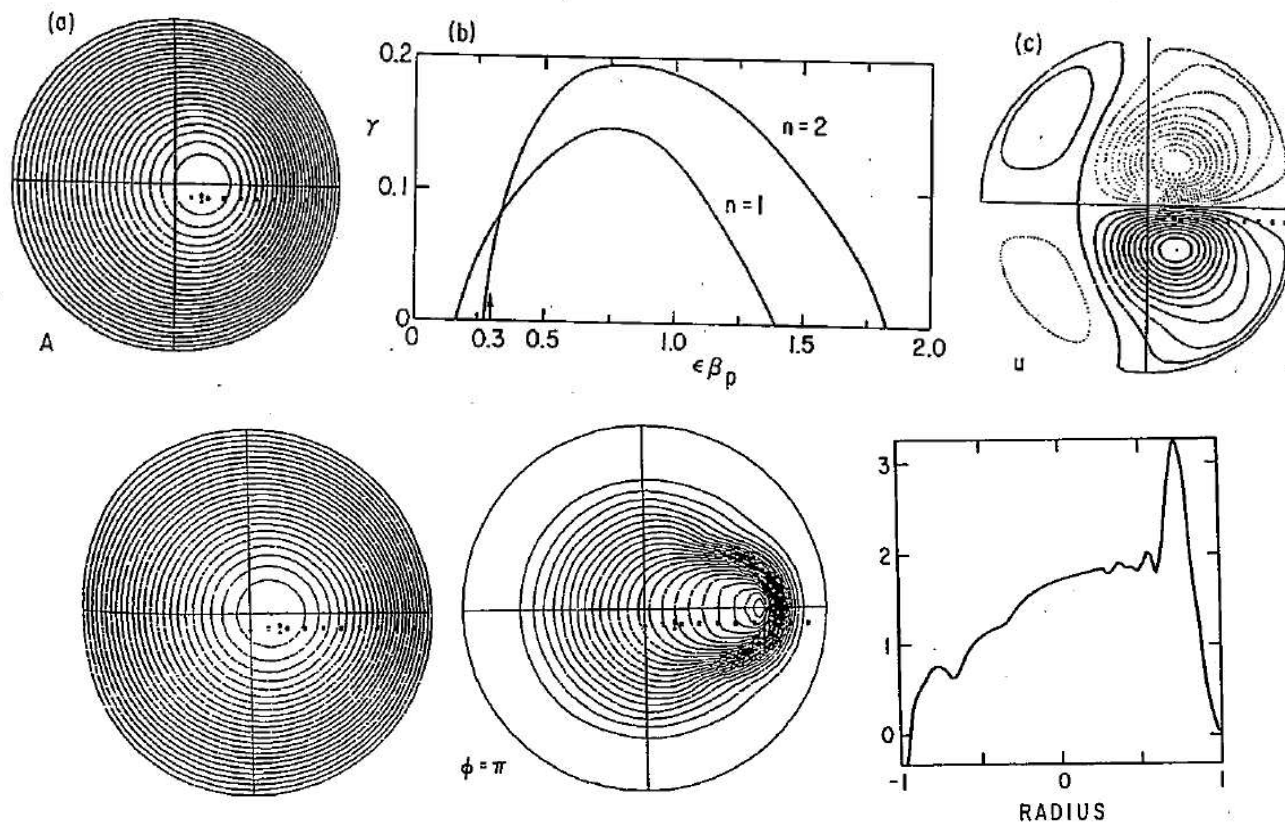
- Shear slab configuration; simulation parameters: $D_I = 0.5$, $S = 10^8$ [Gupta, Callen, and Hegna, APS-DPP 2004].
- Nonlinear LIM saturates; current sheet appears to form.



Saturated state:
$$\nabla^2 \tilde{\psi} \pm \frac{D_I X}{\sqrt{X^2 - 2\tilde{\psi}}} = f\left(\frac{X^2}{2} - \tilde{\psi}\right) \quad [\text{Gupta et al. , 2004}]$$

Current Sheet Formation in Nonlinear Ballooning Simulation

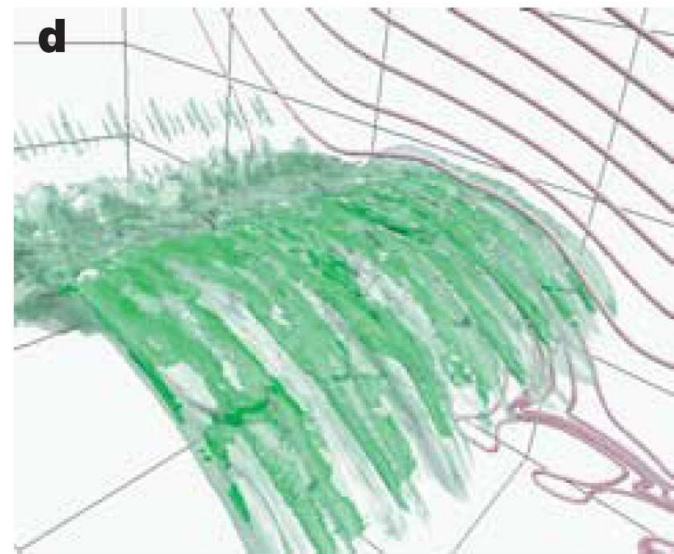
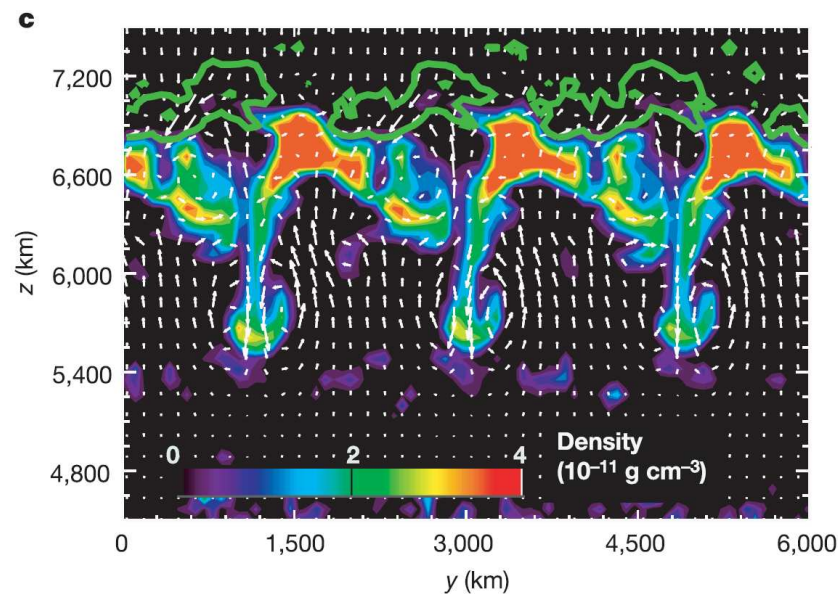
- 3D reduced MHD simulation of high- β , finite aspect-ratio (ϵ) equilibrium: $q_0 = 1$, $\epsilon\beta_p = \beta q^2 / \epsilon = 0.3$ [Monticello *et al.*, IAEA, 1981].



- Fast sawteeth in JET [Edwards *et al.*, 1986] and DIII-D [Lazarus *et al.*, 2006].

Current Sheet Formation from Rayleigh-Taylor Instability

- 3D resistive MHD simulation of emerging solar flux showing the formation of filamentary structure (“finger”) and current sheet formation from magnetic Rayleigh-Taylor instability. [Isobe *et al.*, *Nature*, 2005].
- Emerging solar flux reconnects with pre-existing coronal magnetic field, producing X-ray jets and flares.



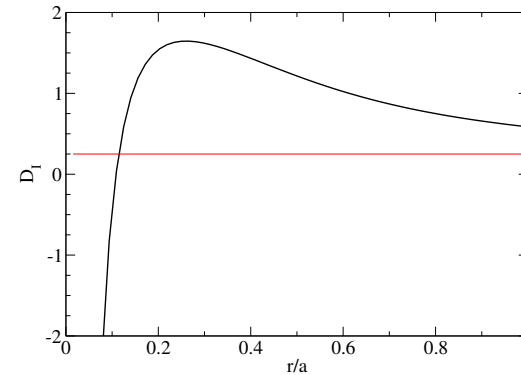
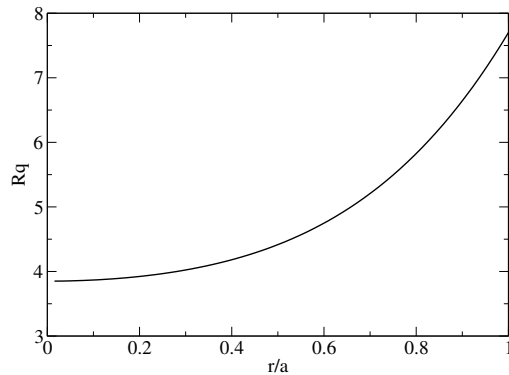
Localized Interchange Mode in a Screw Pinch: Simulation Setup

● Cylindrical configuration

- 1D equilibrium: $\frac{d}{dr} \left(p + \frac{B_z^2 + B_\theta^2}{2} \right) = -\frac{B_\theta^2}{r}$

- $h \equiv \frac{qR}{a} = h_0 \left[1 + h_2 \left(\frac{r}{a} \right)^2 + h_4 \left(\frac{r}{a} \right)^4 \right]$, $p = p_0 \left[1 + p_2 \left(\frac{r}{a} \right)^2 + p_4 \left(\frac{r}{a} \right)^4 \right]$

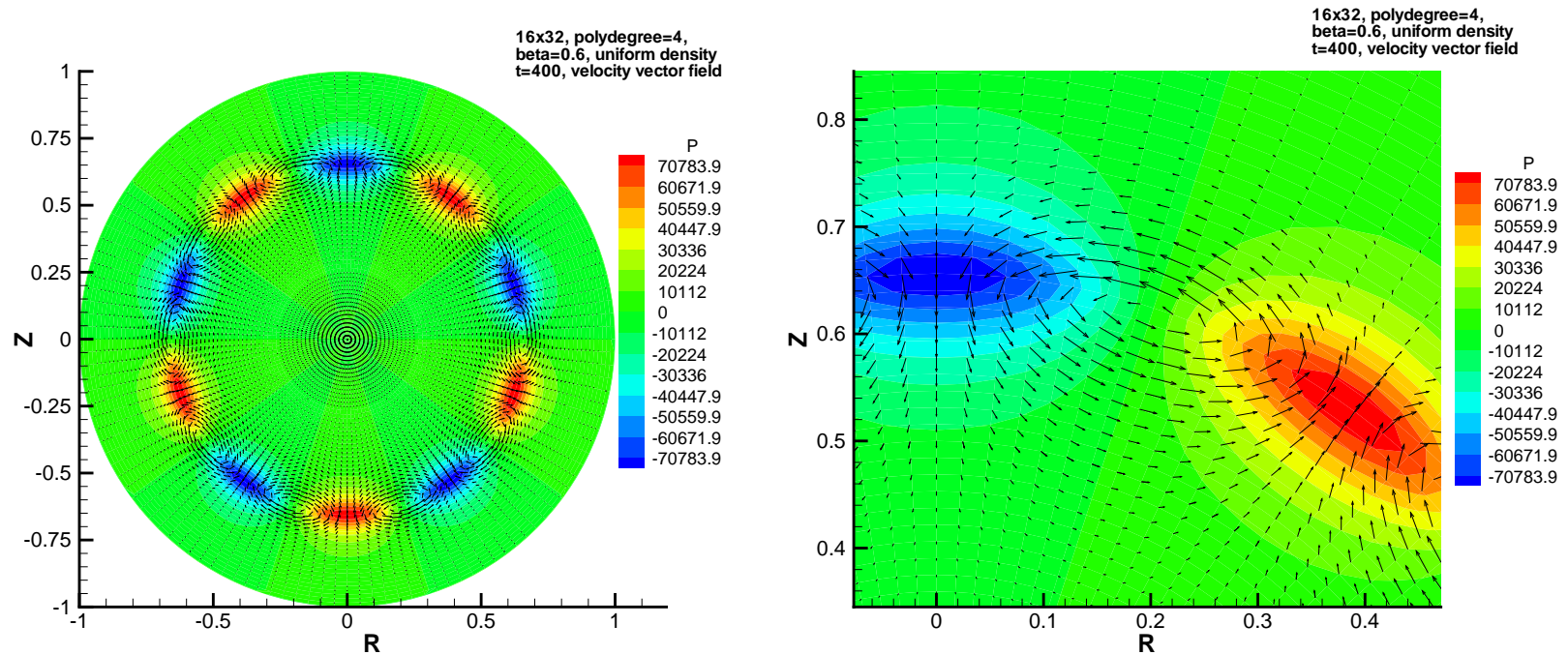
- B_z and current derived from above.



● Initial perturbation

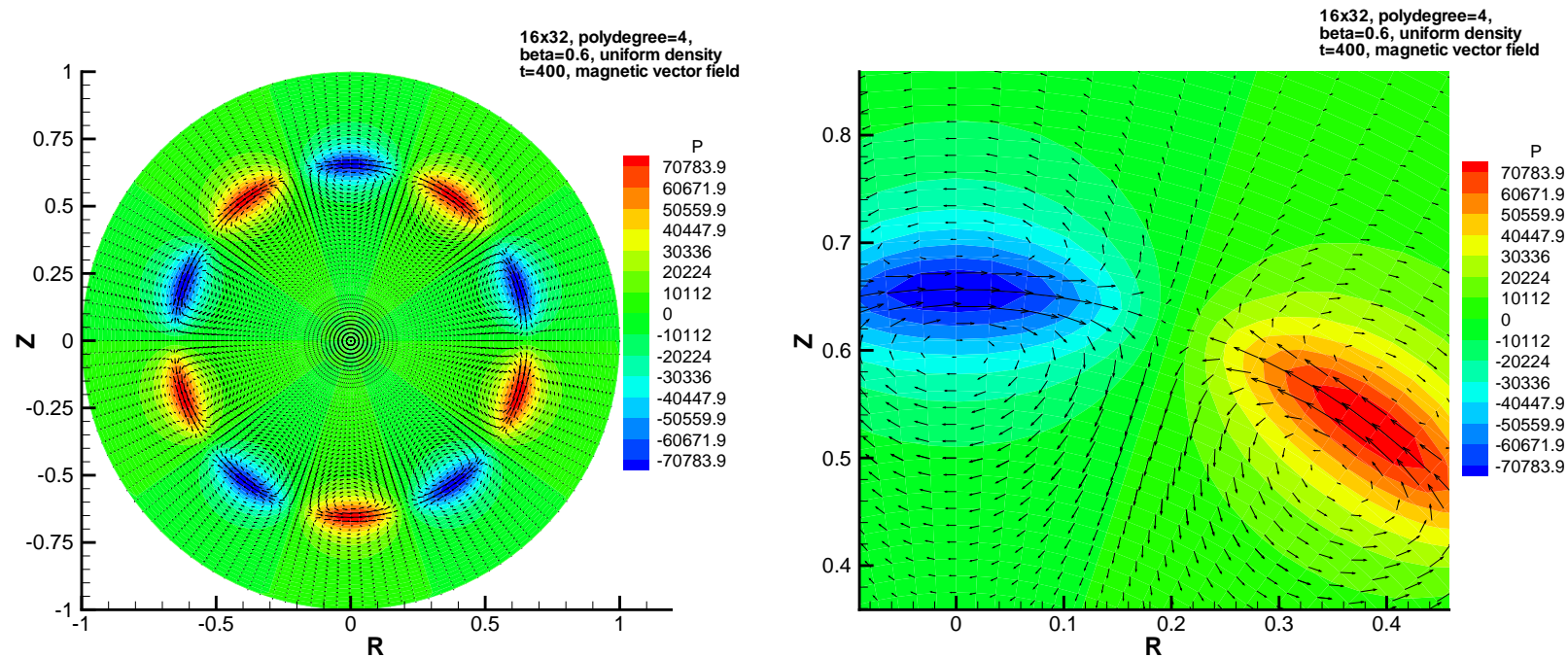
- Shear Alfvén wave: $\mathbf{B}_1 = B_1 \mathbf{e}_\perp$, $\mathbf{u}_1 = u_1 \mathbf{e}_\perp$,
 $\mathbf{e}_\perp = (\mathbf{B}_0 \times \mathbf{k}) / |\mathbf{B}_0 \times \mathbf{k}|$, $u_1 = B_1 / \sqrt{\rho}$

Linear LIM in a Screw Pinch: Pressure and Flow Pattern



- Flow (vector field) and pressure (contour) perturbation localized near $q = 5$ surface.
- Left: full poloidal domain; Right: zoom in of half poloidal period.

Linear LIM in a Screw Pinch: Pressure and Magnetic Pattern



- Magnetic (vector field) and pressure (contour) perturbation localized near $q = 5$ surface.
- Left: full poloidal domain; Right: zoom in of half poloidal period.

Localized Mode vs. Gross Mode [Goedbloed and Sakanaka, POF, 1974]

- Suydam criterion: sufficient/necessary stability condition for the most localized interchange mode: $m, n \rightarrow \infty$ (n : number of radial nodes).
- The most unstable interchange modes are less localized.

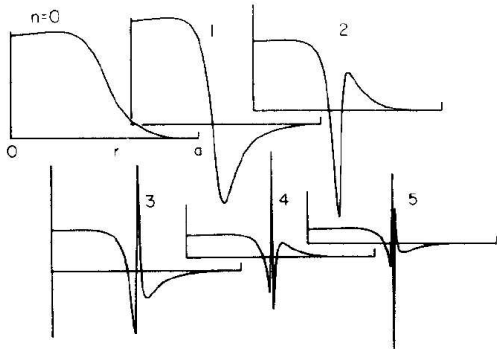


FIG. 4. $m = 1$ Suydam modes for increasing number of nodes.

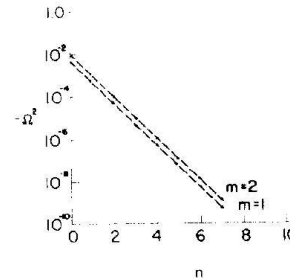


FIG. 6. Growth rate of Suydam modes versus n , for $m = 1$ and 2 modes, $k/m = 0.6$, $a = 0.7$.

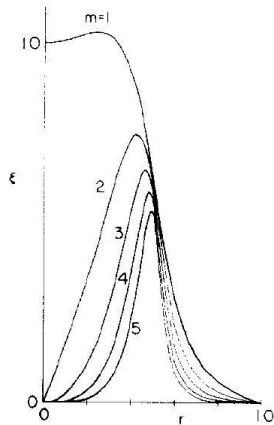
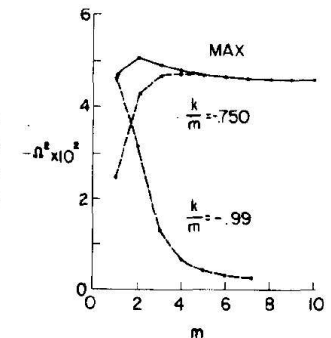
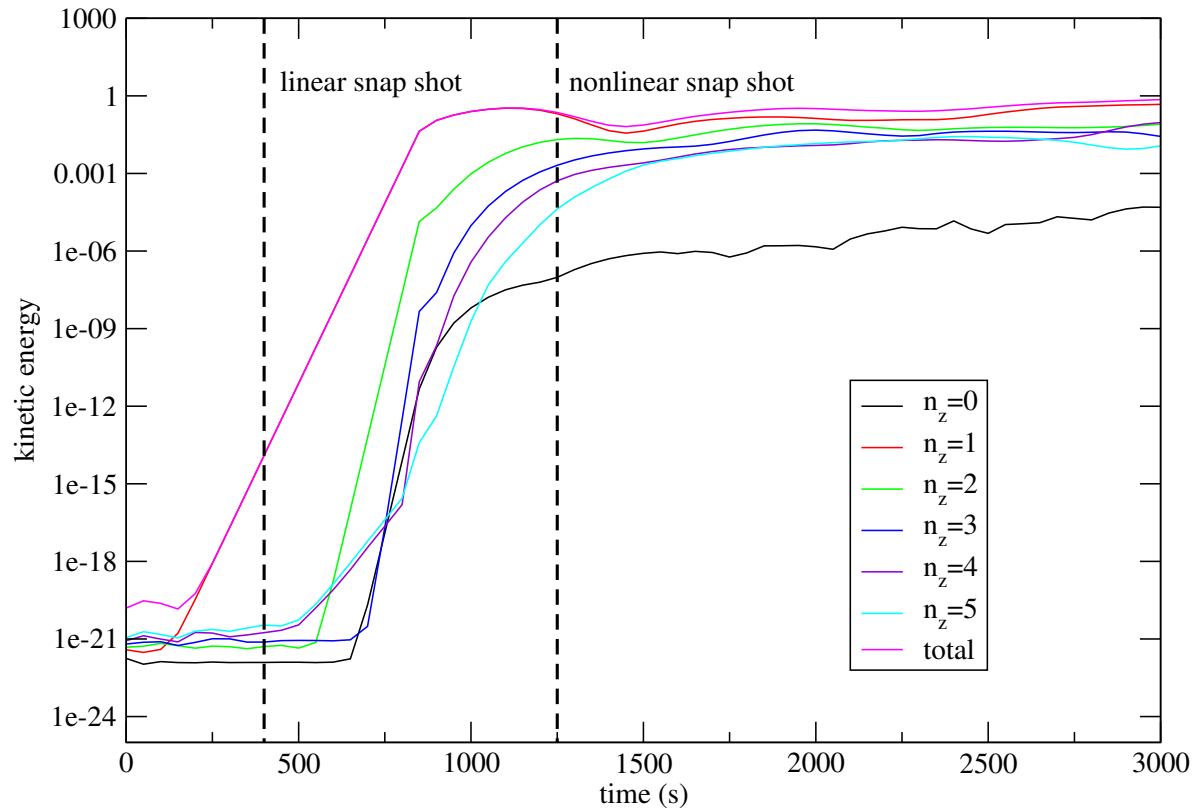


FIG. 5. $n = 0$ Suydam modes for increasing m .

FIG. 7. Growth rate of Suydam modes versus m , for fixed k/m (the dotted lines) and for the values of k where $-\omega^2$ is maximum (the solid line), $a = 0.7$.

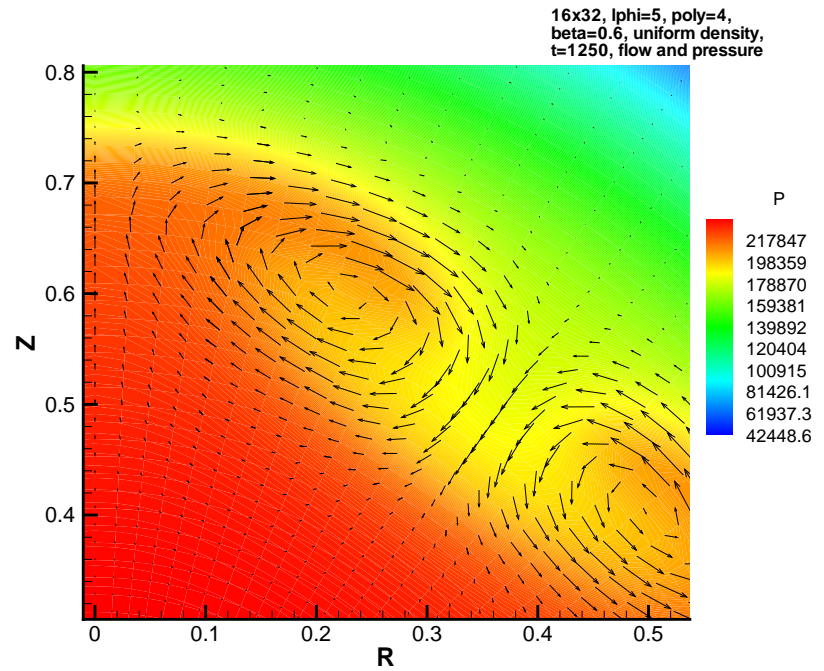
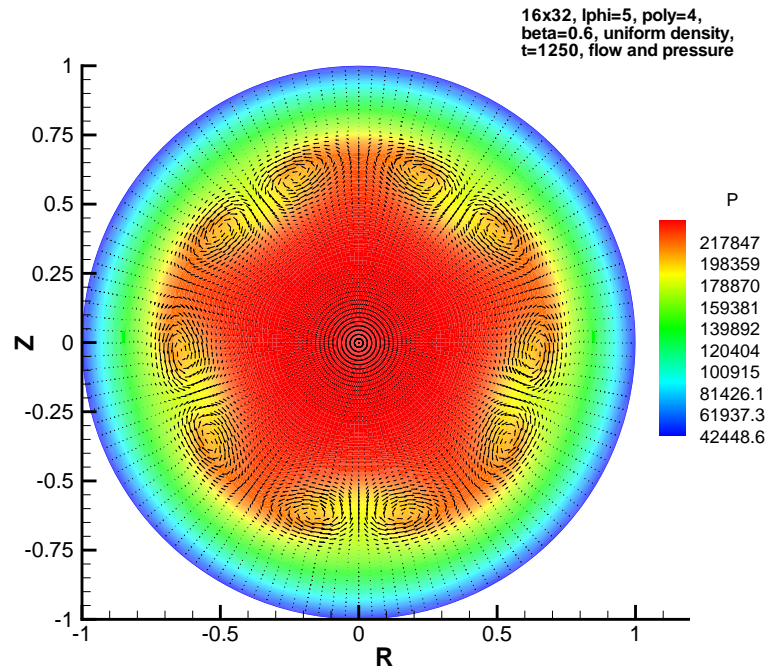


LIM in a Screw Pinch: Nonlinear Growth



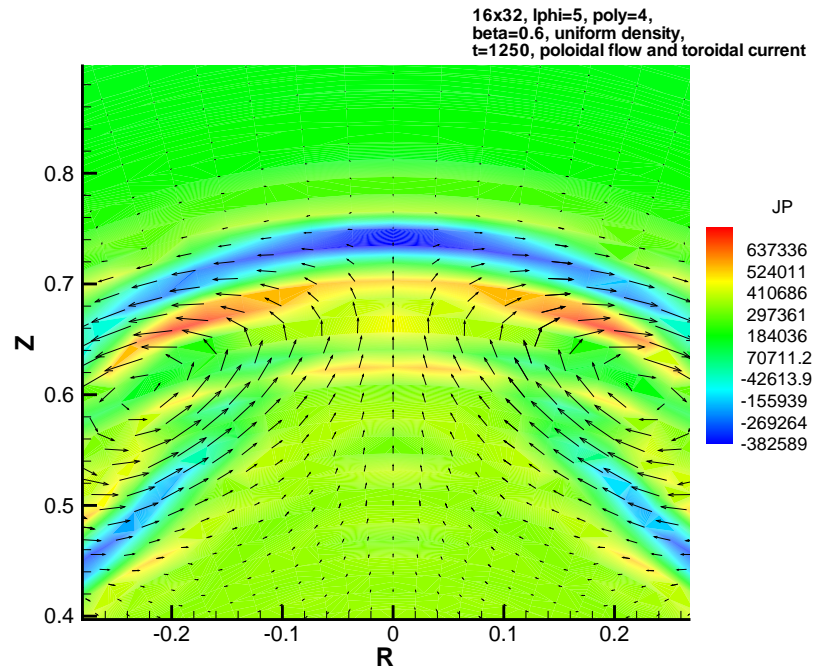
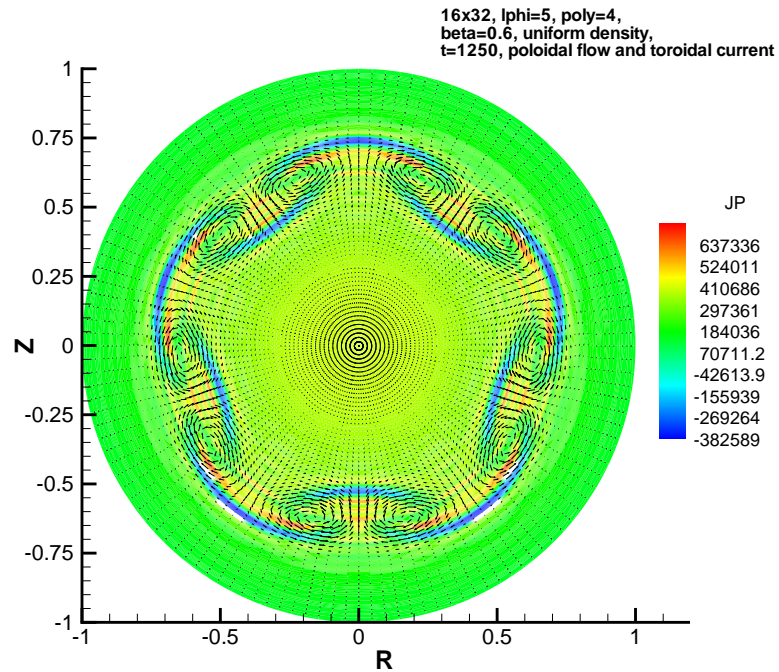
Growth of kinetic energy of the first 6 Fourier (n_z) modes. ($l_{\phi}=5$)

LIM in a Screw Pinch: Nonlinear (Total) Pressure Pattern



Rayleigh-Taylor finger-mushroom pattern formation in pressure contour and flow vector field. Right: zoom in of left panel.

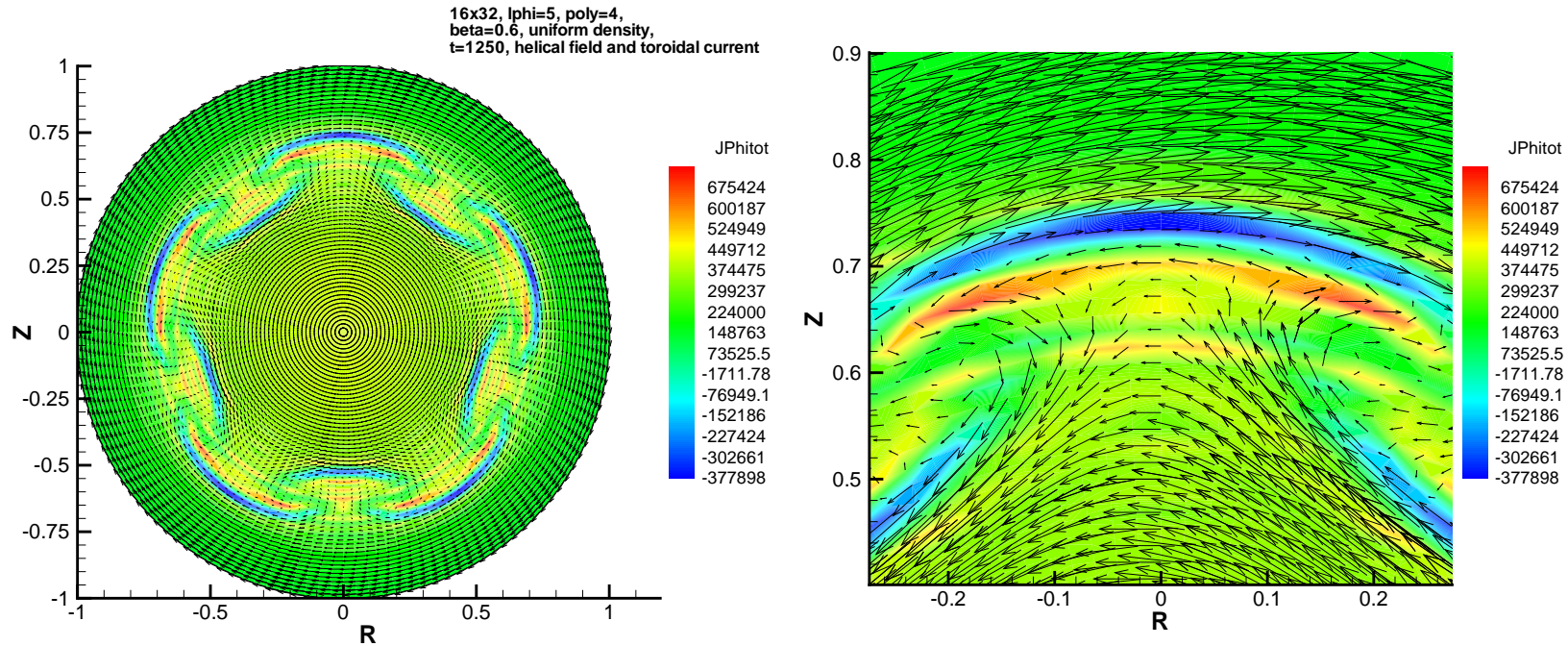
Formation of Current Sheet: J_ϕ and Flow Pattern



Current sheet formation is located at the finger-tip or mushroom-cap of the pressure pattern.

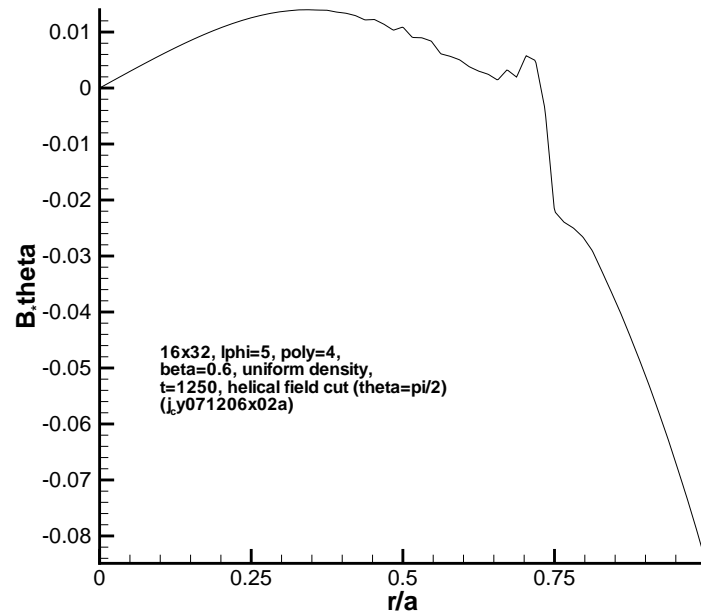
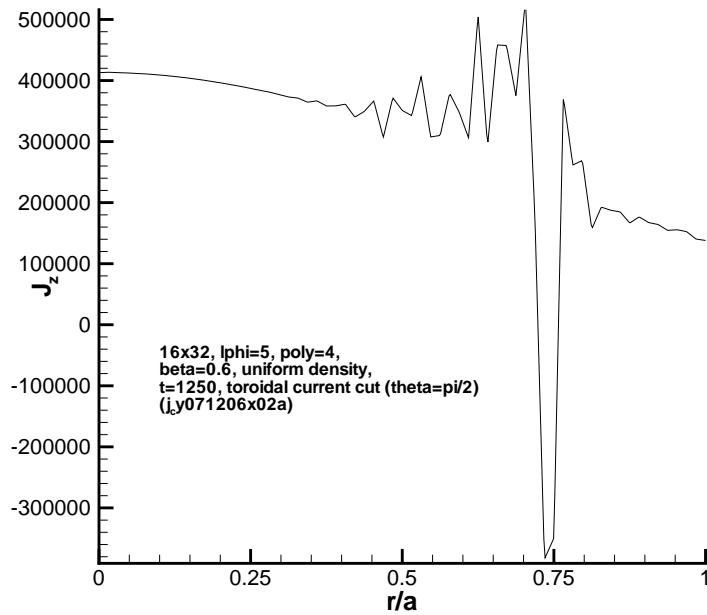
Contour: parallel (toroidal) current; Vector field: flow in poloidal plane.

Formation of Current Sheet: J_ϕ and Helical Field Pattern



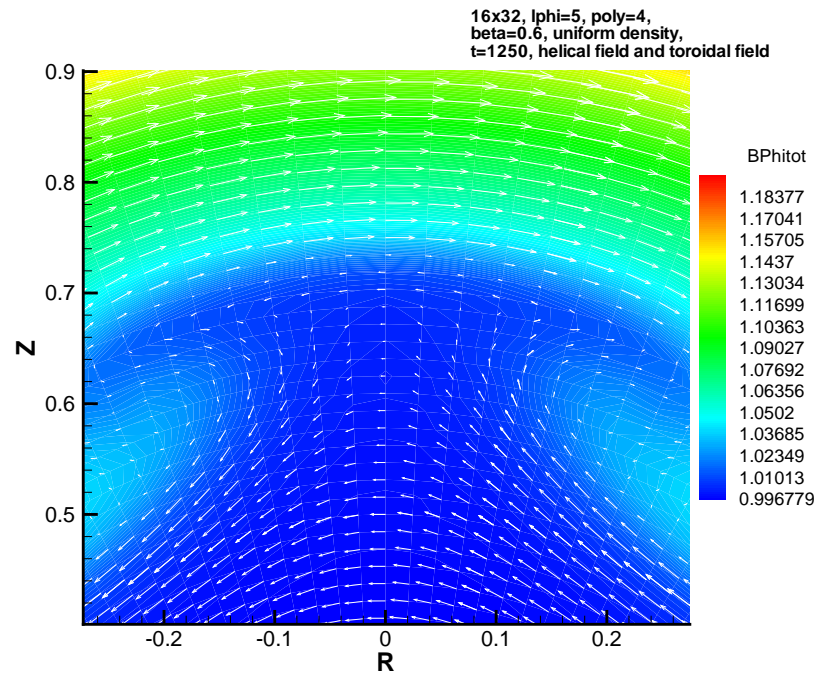
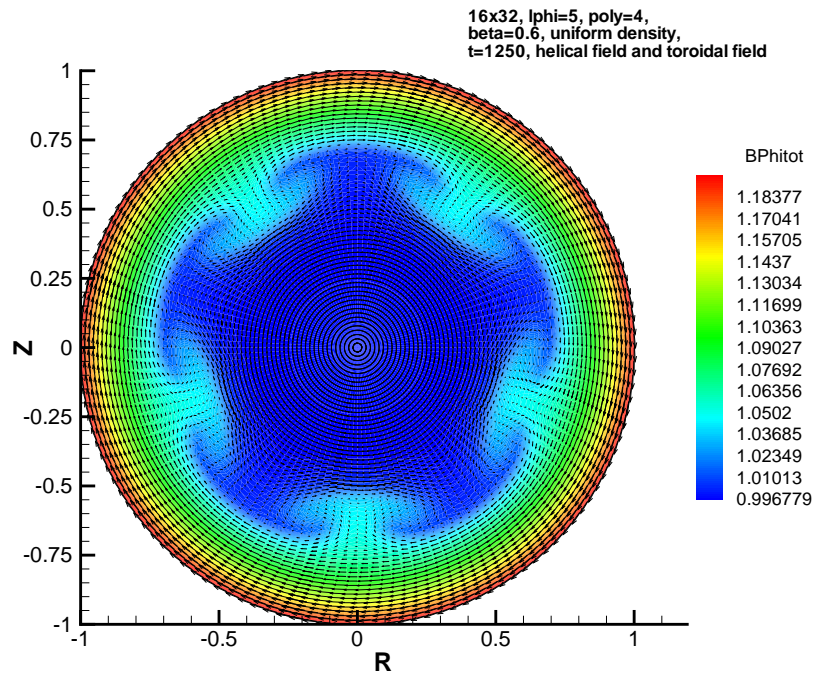
Helical magnetic field:
$$\mathbf{B}_* \equiv \mathbf{B} - \frac{r}{r_s} B_{\theta 0}(r_s) \hat{\theta} - B_\phi(r) \hat{\phi}$$

J_ϕ and Helical Field $B_{*\theta}$ Profiles Across Current Sheet



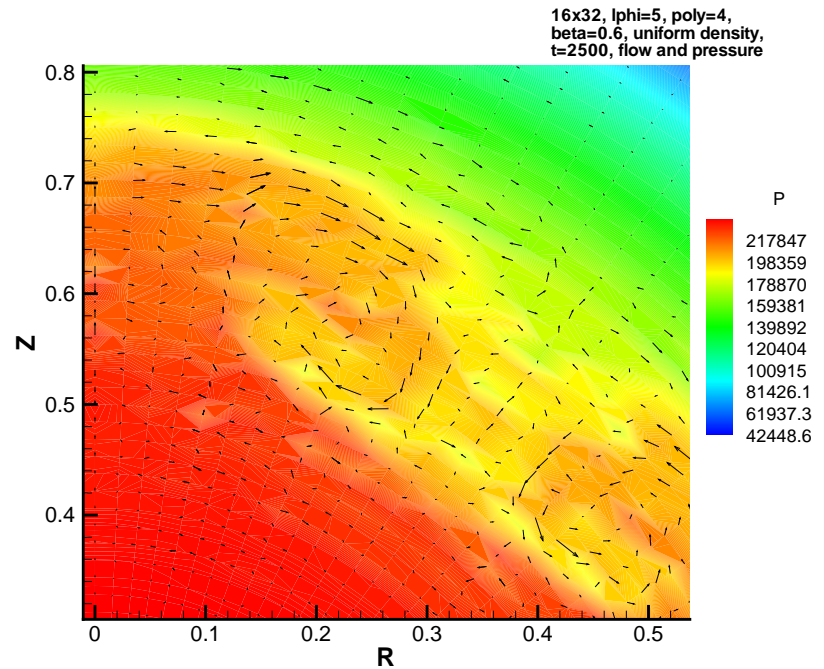
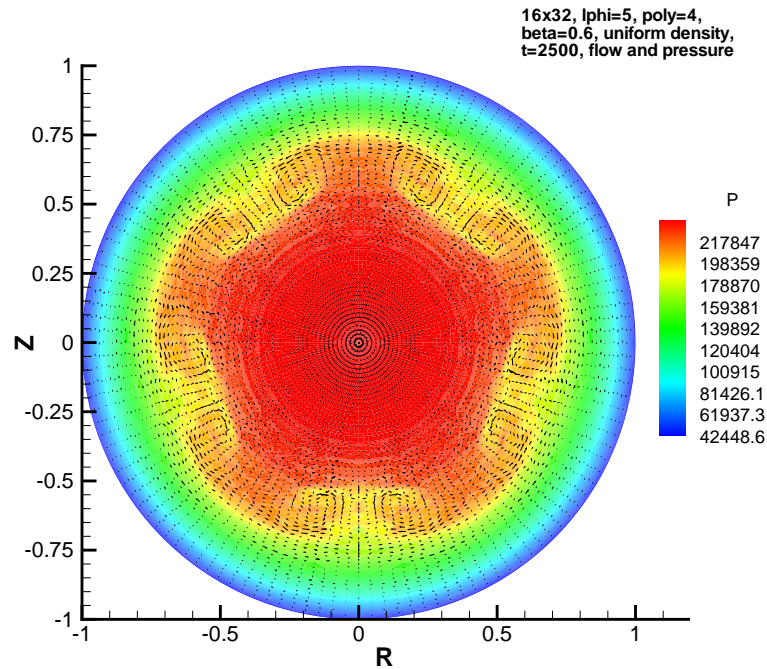
Singularities in J_ϕ and $B_{*\theta}$ profiles indicate the formation of a current sheet.

Toroidal Magnetic (B_ϕ) and Helical Field B_* Pattern



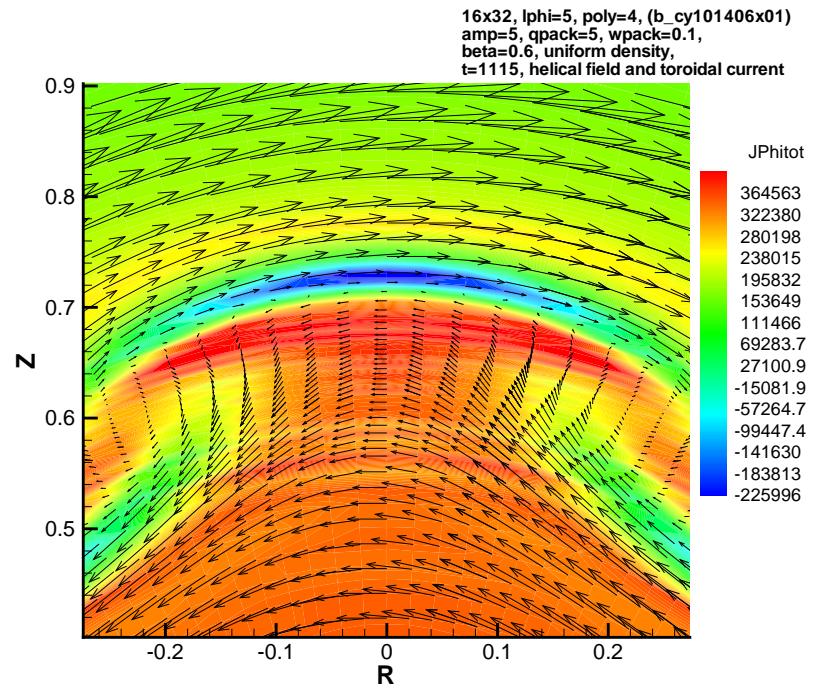
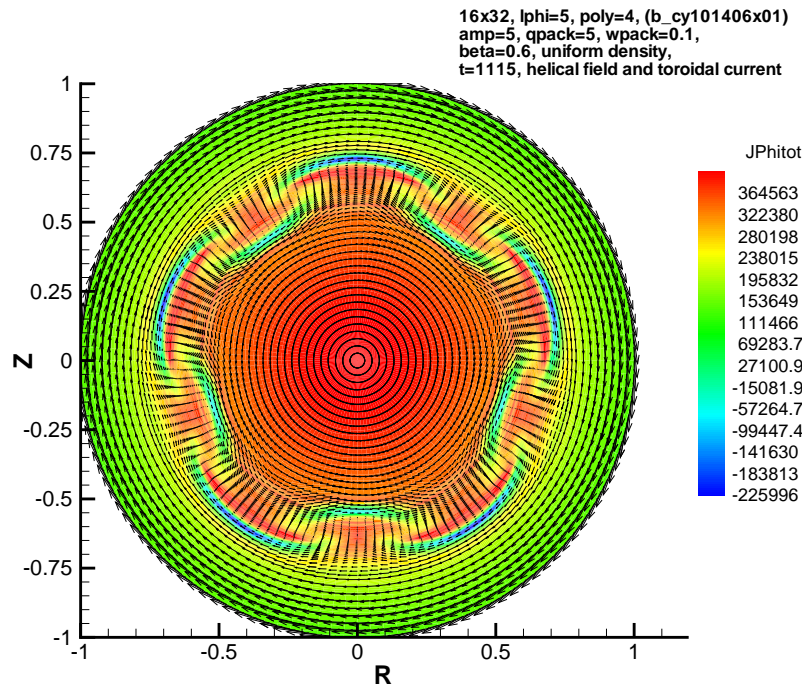
Rayleigh-Taylor finger-mushroom pattern also forms in B_ϕ contour and vector field for B_* .

LIM in a Screw Pinch: Late Nonlinear Phase



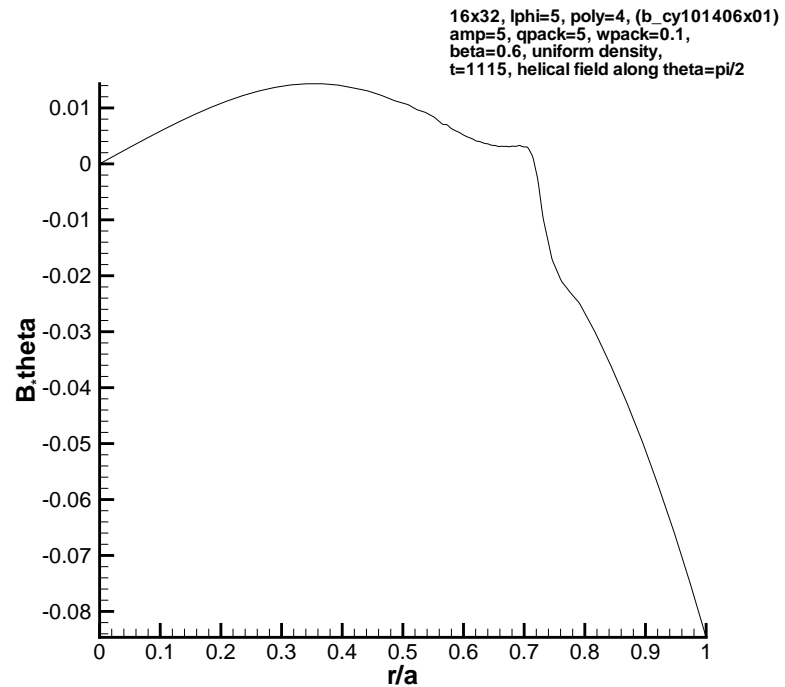
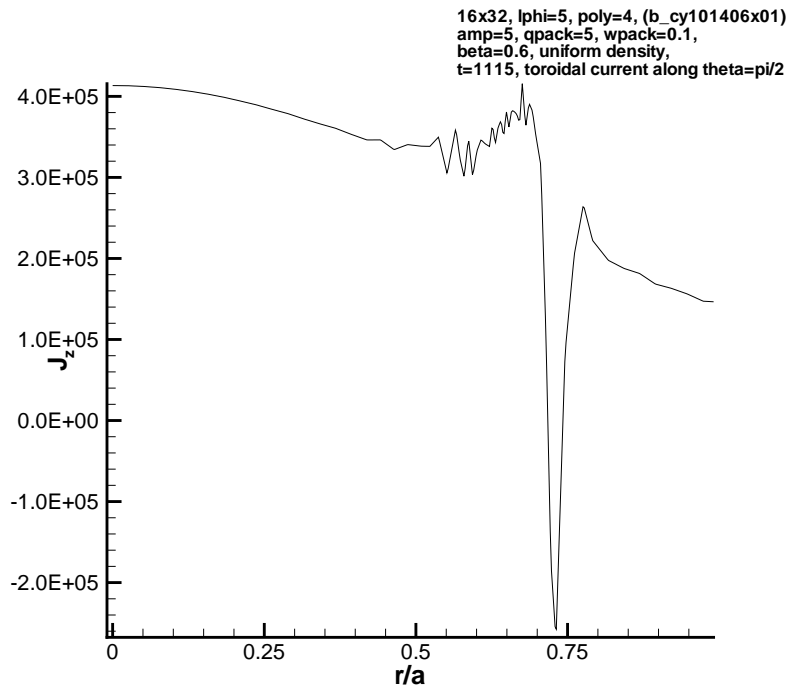
RT finger-mushroom pattern in pressure contour at late nonlinear stage
($t = 2500$) appears more blurred.

Mesh Packing Case: J_ϕ and Helical Field Pattern



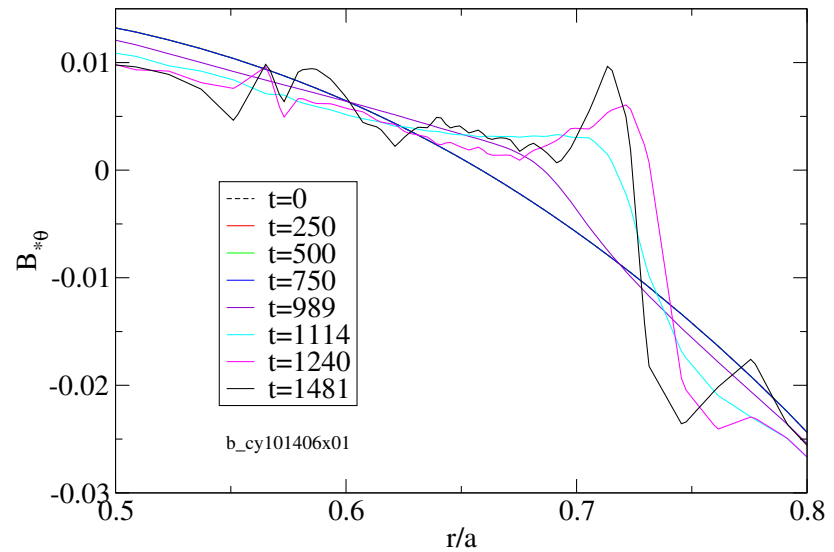
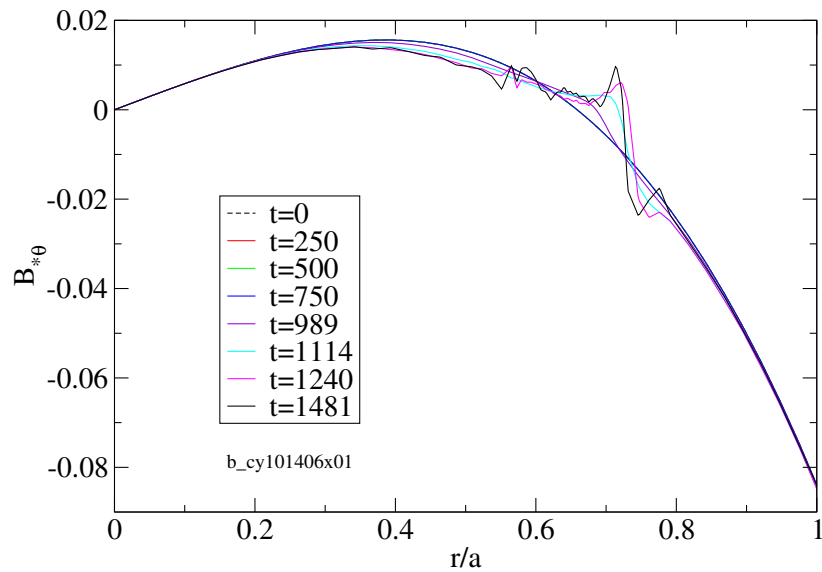
- A non-uniform grid with radial mesh packing near the $q = 5$ surface has been used to better resolve the current sheet structure.
- Contour: toroidal current J_ϕ ; Vector field: helical magnetic field.

Mesh Packing Case: 1D Current Sheet Structure



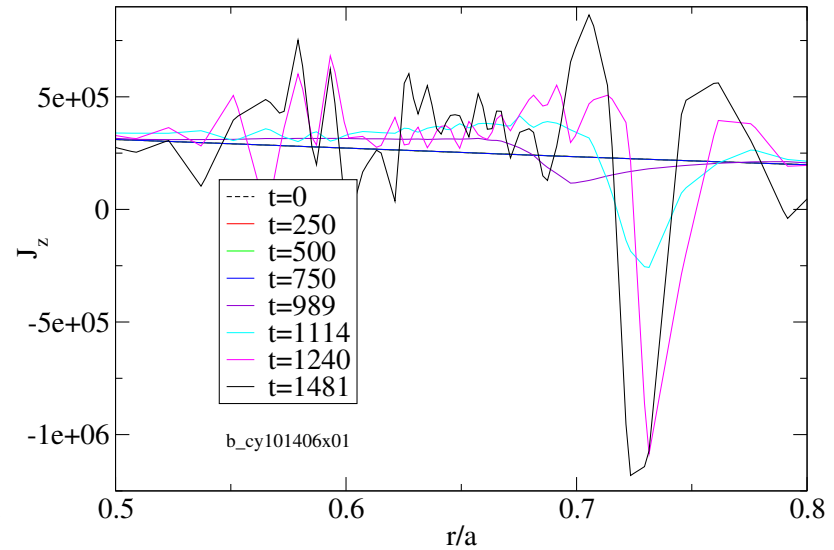
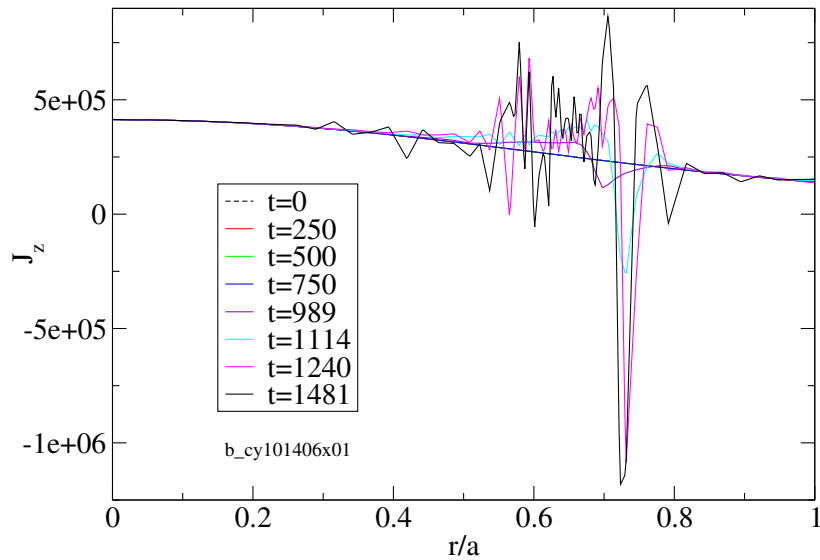
Profiles of toroidal current J_{ϕ} and poloidal helical field $B_{*\theta}$ along a cut through the finger-tip or mushroom-cap of the pressure pattern in a poloidal domain ($\theta = \pi/2$).

Current Sheet Formation Over Time: Poloidal Helical Field $B_{*\theta}$



- Time history of 1D profile of $B_{*\theta}$ along cut $\theta = \pi/2$ across $q = 5$ surface shows the formation of current sheet.
- $t = 0$ to $t = 750$: linear phase; $t \geq 989$ nonlinear phase
- Double/multiple current layers appear to form near late nonlinear phase.

Current Sheet Formation Over Time: Toroidal Current J_ϕ



- Time history of 1D profile of J_ϕ along cut $\theta = \pi/2$ across $q = 5$ surface shows the formation of current sheet.
- $t = 0$ to $t = 750$: linear phase; $t \geq 989$ nonlinear phase
- Double/multiple current layers appear to form near late nonlinear phase.

Current Sheet Formation: Interchange-Tearing Coupling?

Summary (direct consequence of LIM):

- We have investigated nonlinear ideal localized interchange mode (LIM) in a cylindrical configuration with NIMROD simulations.
- Current sheet formations are found in the nonlinear development of localized interchange mode.

Discussion (indirect consequence of LIM):

- Interchange-tearing coupling through current sheet formation and ensuing magnetic reconnection.
- Nonlinear LIM (saturates or continues to grow) may depend on the stability of the current sheet.
- Operational limit or constraint is not set by Suydam (Mercier) criterion alone; interchange-tearing coupling may need be taking into account.